DSCOVR EPIC MAIAC Atmospheric Correction

Science Data Product Guide

Maturity level: Mature

Prepared by

Alexei Lyapustin, NASA GSFC code 613

Yujie Wang, Myungje Choi (NASA GSFC/UMBC)

NASA GSFC

August 18, 2026

TABLE OF CONTENTS

1. INTRODUCTION

1.1 Purpose

This document describes the Level 2G Atmospheric Correction science data products derived with Multi-Angle Implementation of Atmospheric Correction (MAIAC) algorithm from the Earth Polychromatic Imaging Camera (EPIC) onboard the Deep Space Climate Observatory (DSCOVR). MAIAC algorithm was originally developed for MODIS [1] and later adapted for the EPIC processing [2]. The Level 2G means that the products are gridded.

1.2 MAIAC EPIC Overview

The MAIAC EPIC algorithm consists of two parts including standard processing and advanced aerosol characterization. The standard MAIAC processing (Lyapustin et al., 2021a) performs cloud detection that is coupled with detection of absorbing aerosols, retrieval of AOD for cloud-free pixels using the background aerosol model, and an atmospheric correction providing spectral surface bidirectional reflectance factors (BRF) and bidirectional reflectance distribution function (BRDF) model. MAIAC algorithm uses scaled Ross-Thick Li-Sparse (sRTLS) BRDF model (Lyapustin et al., 2025). Compared to standard RTLS model (Wanner et al., 1995), sRTLS adds the Maignan et al. (2004) hot-spot factor to the volumetric kernel, which is important to EPIC given its near hot-spot view geometry, and corrects behavior at high zenith angles above 60°. The background aerosol models for AOD retrievals are defined for nine world regions (Lyapustin et al., 2018) based on climatology analysis of the version 3 AERONET inversion database (Holben et al., 1998; Giles et al., 2023). Using the dynamic time series analysis and the minimum reflectance method, MAIAC also derives the per-pixel spectral regression coefficients (SRC) required for aerosol retrievals. SRC represents spectral ratios of surface reflectance (ρ_{443}/ρ_{680}, ρ_{388}/ρ_{680}, and ρ_{340}/ρ_{388}), where surface reflectance (SR) ρ is a result of Rayleigh and background aerosol atmospheric correction (Lyapustin et al., 2018; 2021a).

The standard processing starts with gridding EPIC's geolocated and calibrated level 1B (L1B) data to 10 km resolution using Zonal Sinusoidal Projection (ZSP) described in Lyapustin et al. (2021a). ZSP minimizes spatial distortions typical to the global Sinusoidal projection. Gridding allows us to, effectively, "observe" the same grid cell over time at different Sun-view angles and perform surface characterization for each grid cell including spectral BRDF, NDVI and SRC. This information, stored for every grid cell, supports detection of clouds and absorbing aerosols, and helps retrievals of aerosol properties. Finally, it's worth mentioning that the MAIAC surface dataset is naturally gap-filled: data from the previous retrievals stay in operational memory for each grid cell until updated from the latest cloud-free observations. Such dynamic update helps MAIAC surface model to adapt to changing land surface conditions, driven by vegetation seasonality, rapid change etc., over time.

Given a reliable characterization of spectral surface reflectance by MAIAC, a well calibrated set of EPIC's vis-NIR (443, 680, 780 nm), UV (340, 388 nm), and atmospheric oxygen absorption (688, 764 nm) channels offers a unique opportunity to simultaneously retrieve AOD, spectral absorption (defined as two parameters: refractive index at 680 nm and spectral absorption exponent; SAE) and height of aerosols. This 4D inversion of EPIC data for 4 aerosol parameters was implemented in MAIAC v3 algorithm (Lyapustin et al., 2025). Further, using spectral imaginary refractive index and AOD, v3 MAIAC infers aerosol composition providing column-integrated volume fraction and mass concentration of black and brown carbon in smoke (Choi et al., 2024; 2025) and of hematite and goethite in aeolian dust (Go et al., 2022; 2025).

The suite of v3 MAIAC EPIC products is summarized in Table 1. It includes atmospherically corrected surface reflectance at 6 different wavelengths; surface BRDF model parameters at four wavelengths (land only), spectral aerosol optical depth (AOD) and single scattering albedo, aerosol fine mode fraction (FMF, ocean only), aerosol layer height, chemical composition of species absorbing in UV-vis, and cloud mask.

Besides geophysical products, the output file also includes the view geometry at the same temporal and spatial resolutions, including Solar Zenith Angle, Solar Azimuth Angle, View Zenith and Azimuth angles (Table. 1).

Table 1: Level 2 MAIAC Geophysical Product Suite

Parameter name	Units	Resolution		Comments
		Temporal	Spatial	
Atmospherically corrected surface reflectance (land); Water-leaving reflectance (ocean)	N/A	65 to 110 min	10 km	The land surface reflectance or water-leaving reflectance over ocean with all atmospheric effects removed. Reported at 340, 388, 443, 551, 680 and 780 nm. The land surface reflectance is retrieved with Lambertian assumption, water-leaving reflectance is a running average of previous and latest values. The update day of water-leaving reflectance is reported in NDVI update day
Rigorous BRDF-coupled atmospherically corrected land surface reflectance (BRF)	N/A	65 to 110 min	10km	Reported at 443, 551, 680 and 780nm.
BRDF model parameters (land only)	N/A	65 to 110 min	10 km	Weights of isotropic, volumetric, and geometric kernels of sRTLS BRDF model. Reported at 443, 551, 680 and 780 nm.
Aerosol optical depth (AOD)	N/A	65 to 110 min	10 km	Aerosol optical depth at 443 and 551 nm
Aerosol fine mode fraction (ocean only)	N/A	65 to 110 min	10 km	The fine mode aerosol fraction over ocean
Angstrom exponent	N/A	65 to 110 min	10 km	Angstrom Exponent at 443-780 nm
AOD (v3 algorithm)	N/A	65 to 110 min	10 km	v3 AOD at 340, 388, 443, 551, 680 and 780 nm
FminAbs (v3 algorithm)	N/A	65 to 110 min	10 km	4D retrieval cost function (residual)
Imaginary Refractive index k_0 (v3 algorithm)	N/A	65 to 110 min	10 km	Imaginary Refractive Index at 680nm
SAE ($k_\lambda = k_0\ (\lambda / \lambda_0)^{-SAE}$) (v3 algorithm)	N/A	65 to 110 min	10 km	Spectral Absorption Exponent defining spectral dependence of imaginary refractive index
Aerosol single scattering albedo (v3 algorithm)	N/A	65 to 110 min	10 km	Aerosol single scattering albedo at 340, 388, 443, 551, 680, 780 nm
Aerosol Layer Height (v3 algorithm)	N/A	65 to 110 min	10 km	Height of aerosol layer above ground in km

VF_Comp1,2; MC_Comp1,2	N/A	65 to 110 min	10 km	Aerosol chemical composition of absorbing species (see Table 5)
Cloud mask	N/A	65 to 110 min	10 km	Cloud mask
Land/Water Mask	N/A	65 to 110 min	10 km	Land, water mask
Solar zenith angle	Degree	65 to 110 min	10 km	Solar zenith angle at the time of observation
Solar azimuth angle	Degree	65 to 110 min	10 km	Solar azimuth angle at the time of observation
View zenith angle	Degree	65 to 110 min	10 km	View zenith angle
View azimuth angle	Degree	65 to 110 min	10 km	View azimuth angle
NDVI	N/A	65 to 110 min	10 km	Running average of normalized difference vegetation index
NDVI/water-leaving reflectance updated day	N/A	65 to 110 min	10 km	Date of last update of NDVI/water leaving reflectance
Quality Assessment (QA)	N/A	65 to 110 min	10 km	Overall quality of the MAIAC retrievals

MAIAC uses time series analysis observing the same surface grid cell over time in order to characterize surface spectral BRDF and improve cloud detection, aerosol retrieval and atmospheric correction. To this end, MAIAC processing starts with gridding EPIC L1B data to 10 km zonal sinusoidal grid. All products are derived and reported at 10 km resolution and written in the standard Hierarchical Data Format 5 (HDF5) using HDF-defined data models (http://www.hdfgroup.org/HDF5/). The EPIC MAIAC data products are publicly available from the NASA Langley Atmospheric Science Data Center (https://asdc.larc.nasa.gov/project/DSCOVR/DSCOVR_EPIC_L2_MAIAC_03).

1.3 Product maturity level

MAIAC EPIC atmospheric aerosol products have been globally validated for the entire mission period using AERONET (AOD, spectral SSA) and CALIOP CALIPSO (aerosol layer height (ALH)) data (Lyapustin et al., 2023; 2025). The aerosol composition products (volume fraction and mass concentration of black and brown carbon in smoke (Choi et al., 2024) and of hematite and goethite in aeolian dust (Go et al., 2022) were validated against available field campaign and in-situ, and via comparisons with other composition products. The validation showed a good-to-high accuracy of MAIAC atmospheric product suite, in particular for spectral SSA and height.

The high quality of MAIAC EPIC surface reflectance product suite (BRF, BRDF, NDVI) has been recognized though extensive analysis in the follow-on retrievals deriving LAI, FPAR, sunlit LAI (SLAI) etc. higher-level vegetation products. This categorizes MAIAC EPIC v3 algorithm and product suite as ***mature and globally validated***.

1.4 DSCOVR EPIC documents

Project documents are available at https://asdc.larc.nasa.gov/project/DSCOVR. DSCOVR EPIC publications can be found at https://epic.gsfc.nasa.gov/science/pubs. Below is a list of publications describing MAIAC EPIC algorithms and products.

Choi, M., Lyapustin, A., Schuster, G. L., Go, S., Wang, Y., Korkin, S., et al. (2024). Light-absorbing black carbon and brown carbon components of smoke aerosol from DSCOVR EPIC measurements over North America and central Africa. *Atmos. Chem. Phys.* 24, 10543–10565. doi: 10.5194/acp-24-10543-2024

Choi M., Lyapustin A., Wang Y., Hyer E.J., Eck T.F. and Korkin S. (2025) Climatology and variability of smoke aerosols from MAIAC EPIC observations over North America (2016–2024). *Front. Remote Sens*. 6:1654779. doi: 10.3389/frsen.2025.1654779.

Go, S., Lyapustin, A., Schuster, G. L., Choi, M., Ginoux, P., Chin, M., Kalashnikova, O., Dubovik, O., Kim, J., da Silva, A., Holben, B., and Reid, J. S.: Inferring iron-oxide species content in atmospheric mineral dust from DSCOVR EPIC observations, *Atmos. Chem. Phys*., 22, 1395–1423, https://doi.org/10.5194/acp-22-1395-2022, 2022.

Go S., Lyapustin A., Choi M., Korkin S., Wang Y. and Hyer E.J. (2025) MAIAC-based climatology of atmospheric iron-oxide dust species from DSCOVR EPIC observations. *Front. Remote Sens.* 6:1676851. doi: 10.3389/frsen.2025.1676851.

Lyapustin, A., Wang, Y., Korkin, S., and Huang, D. (2018). MODIS Collection 6 MAIAC algorithm. *Atmos. Meas. Tech.* 11, 5741–5765. doi: 10.5194/amt-11-5741-2018

Lyapustin, A., Go, S., Korkin, S., Wang, Y., Torres, O., Jethva, H., et al. (2021). Retrievals of Aerosol Optical Depth and Spectral Absorption From DSCOVR EPIC. *Front. Remote Sens.* 2, 1–14. doi: 10.3389/frsen.2021.645794

Lyapustin, A., Wang, Y., Go, S., Choi, M., Korkin, S., Huang, D., et al. (2021). Atmospheric Correction of DSCOVR EPIC: Version 2 MAIAC Algorithm. *Front. Remote Sens.* 2. doi: 10.3389/frsen.2021.748362

Lyapustin A., Choi M., Wang Y., Korkin S., Hyer E. and Marshak A. (2025) Simultaneous retrieval of aerosol optical depth, spectral absorption and layer height from DSCOVR EPIC using MAIAC algorithm. *Front. Remote Sens*. 6:1677438. doi: 10.3389/frsen.2025.1677438.

Lyapustin A., Marshak A. and Szabo A. (2026) Editorial: Earth observations from the deep space: 10 years of the DSCOVR mission. Front. Remote Sens. 7:1810164. doi: 10.3389/frsen.2026.1810164.

Marshak A, Lyapustin A, Schuster GL, Szabo A and Eckman R (2022) Editorial: DSCOVR EPIC/NISTAR: 5 Years of Observing Earth From the First Lagrangian Point. *Front. Remote Sens.* 3:963660. doi: 10.3389/frsen.2022.963660

Vasilkov, A., A. Lyapustin, B.G. Mitchell, D. Huang, UV Reflectance of the Ocean from DSCOVR/EPIC: Comparisons with a Theoretical Model and Aura/OMI Observations, *J. Atmos. Oceanic Technology*, 2087-2099, Nov. 2019, https://doi.org/10.1175/JTECH-D-18-0150.1.

An overview of the DSCOVR EPIC project can be found in

Marshak, A., Herman, J., Szabo, A., Blank, K., Carn, S., Cede, A., et al. (2018). Earth observations from DSCOVR epic instrument. *Bull. Am. Meteorol. Soc.* 99, 1829–1850. doi: 10.1175/BAMS-D-17-0223.1

2. EXPERIMENT OVERVIEW

The DSCOVR mission is a multiagency (National Oceanic and Atmospheric Administration [NOAA], U.S. Air Force, and NASA) mission launched from Cape Canaveral, Florida on February 11, 2015 with the primary goal of making unique space weather measurements from the first Sun-Earth Lagrange point (L1). The L1 point is on the direct line between Earth and the Sun located ~1.5 million km sunward from Earth. The spacecraft is orbiting this point in a six month Lissajous orbit with a Sun-Earth-View (SEV) angle varying between 1.5°

and 11.5°. The primary science objective of the DSCOVR mission is to provide solar wind thermal plasma and magnetic field measurements to enable space weather forecasting by NOAA.

The DSCOVR hosts NASA Earth-Observing Instrument, the Earth Polychromatic Imaging Camera (EPIC). The EPIC measures solar radiation reflected by Earth in ten narrowband spectral intervals and delivers images of the sunlit side of Earth for science applications.

2.1. EPIC instrument characteristics

The EPIC instrument collects multispectral data of the Earth in ten wavelengths. The spectral bands are summarized in Table 2.

Table 2: EPIC spectral band composition

Wavelength, nm	FWHM, nm	Nominal Product
317.5±0.1	1±0.2	Ozone
325±0.1	2±0.2	Ozone
340±0.3	3±0.6	Ozone, Aerosols, Clouds
388±0.3	3±0.6	Aerosols, Clouds
443±1	3±0.6	Aerosols
551±1	3±0.6	Aerosols, Vegetation
680±0.2	2±0.4	Aerosols, Vegetation, Clouds,O_2 B-Band Reference
687.75±0.2	0.8±0.2	O_2 B-Band Cloud Height, Aerosol Height
764±0.2	1±0.2	O_2 A-Band Cloud Height, Aerosol Height
779±0.3	2±0.4	O_2 A-Band Reference, Vegetation

2.2. Rationale for the DSCOVR EPIC MAIAC product

Atmospherically corrected surface reflectance and surface BRDF are important quantities for climate modeling and study of global land, land use and land change. Aerosol radiative effects and their interactions with clouds are associated with significant uncertainties in the climate models; aerosol amount and properties are important for the air quality and human health research and monitoring.

3. EPIC SUN-SENSOR GEOMETRY

The sun-sensor geometry is expressed in a right-handed coordinate system in which the Z-axis (shown as "+Z" in Fig. 1) is aligned with the normal to the surface reference ellipsoid (defined by the World Geodetic System 1984, WGS84), and points toward the center of the Earth. The X-axis points toward the North Pole and the Y-axis points to east.

The Sun and sensor positions are represented by unit vectors Ω_0 and Ω directed *downward* from the *Sun to target* (i.e., point at the Earth surface) and from *sensor to target*, respectively. Their polar (θ_0 and θ) and azimuthal (φ_0 and φ) angles are given in the right-handed coordinate system (Fig. 1). Their ranges are between 0 and 90° (polar angles) and between 0 and 360° (azimuthal angles). In this coordinate system the Solar Zenith Angle (SZA, the angle between the target-to-Sun direction, $-\Omega_0$, and the –Z axis) coincides with the polar angle of Ω_0, i.e., $\theta_0 = SZA$.

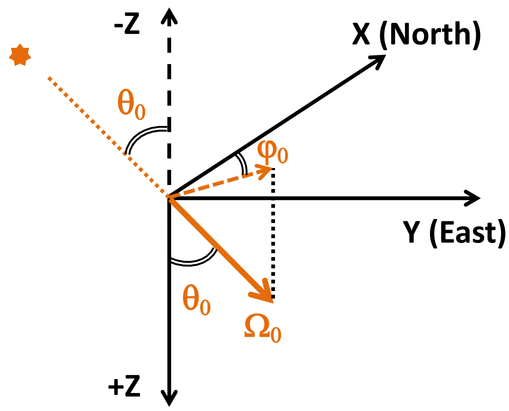

Figure 1. Right-handed coordinate system in which the Z-axis (shown as "+Z") points toward the center of the Earth. The X-axis and Y-axis point toward the North and East, respectively. The direction (unit vector) Ω_0 has an azimuthal angle, φ_0 , measured clockwise from the local north vector (X) to the projection of Ω_0 onto the XY plane, and a polar angle, θ_0, with respect to the +Z axis.

The Earth-observing geometry of the EPIC instrument is characterized by a nearly constant phase angle (the angle between directions to the Sun and to the sensor) between 4.5° and 11.5°. The phase angle, γ, can be calculated as

$$\gamma = \mathrm{acos}(\cos\theta\cos\theta_0 + \sin\theta\sin\theta_0\cos(\varphi - \varphi_0)). \tag{1}$$

4. PRODUCT TILING

In MAIAC product, globe is divided into 4 zones along the east-west direction, and 2 vertical tiles along the north-south axes (Fig. 2). Each tile is identified by its zone number (from 0 to 3) and vertical tile number (from 0 to 1) coordinates, e.g., tile01 represents zone 0 and tile 1. Each tile contains 1000x1000 pixels.

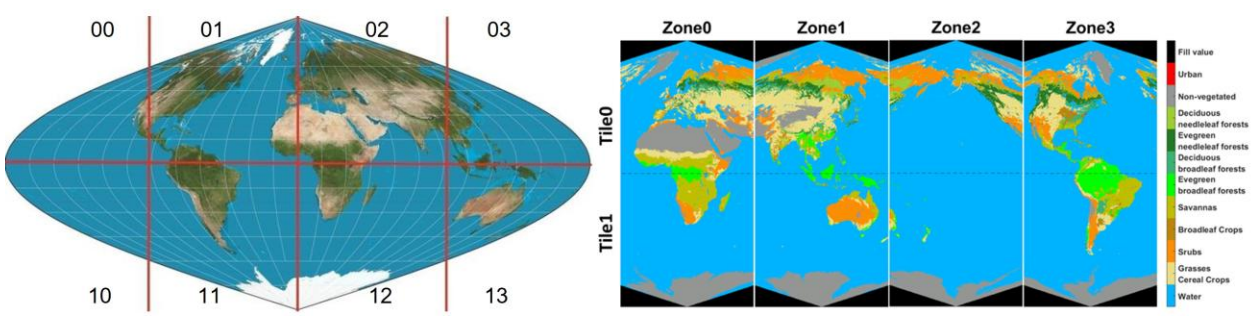

Figure 2. (left) Global Sinusoidal projection in v1 MAIAC, and (right) Zonal Sinusoidal projection with global land cover types in versions v2-v3. The right figure shows EPIC MAIAC global tiles and landcover map in 10 km resolution grid. The globe is divided into 4 zones and each zone is divided into 2 tiles. Each tile is identified by its zone number (from 0 to 3) and vertical tile number (from 0 to 1).

5. LEVEL 2 MAIAC PRODUCT

The Level 2 EPIC MAIAC product uses rotated and zoned Sinusoidal projection with a 10 km grid size. The central meridian of each zone is shown in table 3. To reduce the size of our final product, we do not include the pixel level geolocation in the MAIAC data product. Instead, we provide an ancillary data file that provides the latitude and longitude of each pixel and the ancillary data file can be accessed from the following link: https://portal.nccs.nasa.gov/datashare/maiac/DataRelease/EPICTile_lat-lon/

Table 3. Zones of MAIAC products

Zone name	Central meridian of SIN projection	Meridian of left bound	Meridian of right bound
Zone 0	20	-25	65
Zone 1	110	65	155
Zone 2	-160	155	-115
Zone 3	-70	-115	-25

5.1. MAIAC product file name

The file name has the following format:

DSCOVR_EPIC_L2_MAIAC_V2_YYYYMMDDHHMMSS_V2.h5

Here V1=02 and V2=03 are versions of the MAIAC product and of L1B top of atmosphere (TOA) reflectance data, respectively. Current version is V2. YYYYMMDDHHMMSS gives the date and GMT time of EPIC image acquisition. For example, file DSCOVR_EPIC_L2_MAIAC_03_20160823141930_03.h5 contains MAIAC parameters for an EPIC image acquired on August 23, 2016 (20160823) at 14h10m30s GMT (141930).

5.2. HDF file structure

The MAIAC product is distributed as standard Hierarchical Data Format 5 (HDF5) file. To reduce the size of the final data product, the data are compressed using the default lossless gzip option provided by the Python HDF5 package called h5py. On average, the L2 MAIAC compressed product is about 20 megabytes (MB) in size, with compression giving 7-10-fold reduction of the file size.

In the HDF5 file, data are grouped by tiles. Each group contains geophysical parameters, associated quality assessment variables (QA and Sur_refl_uncertainty) and sun-sensor geometry. The root group directory contains a set of attributes that describes the content of the HDF5 file. Figure 3 illustrates a snapshot of the layout of a L2 MAIAC product.

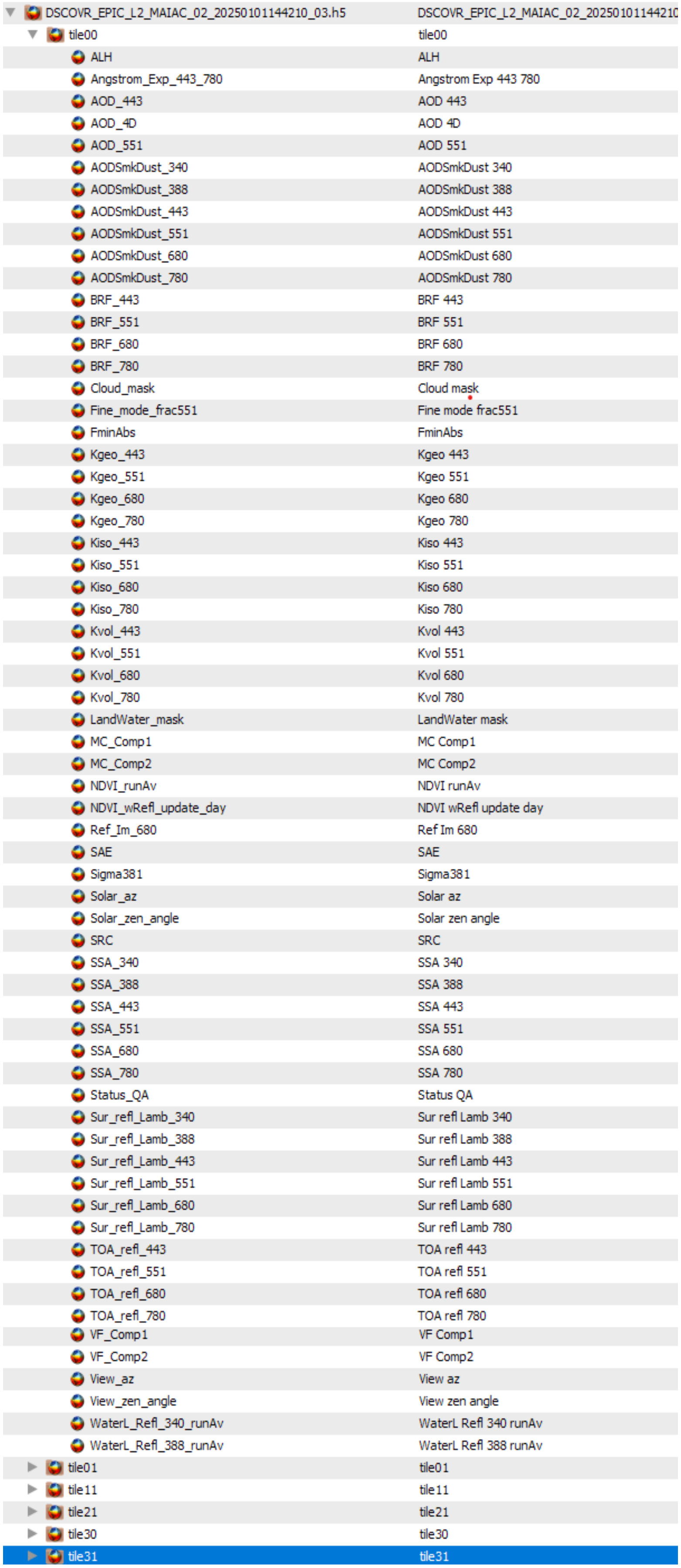

Figure 3. Structure of the L2 MAIAC product. Data are grouped by tiles. Each group contains geophysical parameters (aerosol properties, atmospherically corrected surface reflectance, surface BRDF model parameters, TOA reflectance, and cloud mask), associated quality assessment variables, and sun-sensor geometry.

5.3. Root attributes

Root attributes include date and time of the EPIC image acquisition, fill values, parameter's valid ranges, map projection, scale factors and list of tiles present in the file. Details are summarized in Table 3.

Table 4: Root attributes of the Level 2 EPIC MAIAC product

Attribute name	Value	Type	Description
Map projection	10 km Zonal SIN, center meridians are 20, 110, -160, -70 degree	string	In each zone, parameters are projected on 10 km sinusoidal grid
Fill_value	-9999	16 bit integer	Parameter was not generated
Out_of_bound_value	-9998	16 bit integer	out of map boundary
Toa_refl_scale_factor	0.0001	32 bit floating point	the scale factor to convert a DN value to TOA reflectance
Sur_refl_scale_factor	0.0001	32 bit floating point	the scale factor to convert a DN value to surface reflectance
AOD_scale_factor	0.0001	32 bit floating point	the scale factor to convert a DN value to aerosol optical depth
Fine_mode_frac_scale_factor	0.0001	32 bit floating point	the scale factor to convert a DN value to aerosol fine mode fraction
Ref_Im_scale_factor	0.0001	32 bit floating point	the scale factor to convert a DN value to the uncertainty of surface reflectance
AAE_scale_factor	0.001	32 bit floating point	the scale factor to convert a DN value to SAE
RMSE_scale_factor	0.0001	32 bit floating point	the scale factor to convert a DN value to RMSE of AOD with flexible model, FminAbs
SSA_scale_factor	0.0001	32 bit floating point	the scale factor to convert a DN value to the uncertainty of surface reflectance
Angle_scale_factor	1.0	32 bit floating point	Sun-sensor geometry parameters should be multiplied by the scale factor to get their physical value
tile00_present	0,1	8 bit integer	Indicates if tile00 present (value=1) in dataset
tile01_present	0,1	8 bit integer	Indicates if tile01 present (value=1) in dataset
tile10_present	0,1	8 bit integer	Indicates if tile02 present (value=1) in dataset
tile11_present	0,1	8 bit integer	Indicates if tile03 present (value=1) in dataset
tile20_present	0,1	8 bit integer	Indicates if tile10 present (value=1) in data et

tile21_present	0,1	8 bit integer	Indicates if tile11 present (value=1) in dataset
tile30_present	0,1	8 bit integer	Indicates if tile12 present (value=1) in data et
tile31_present	0,1	8 bit integer	Indicates if tile13 present (value=1) in dataset

5.4. Datasets

Each group contains geophysical parameters, associated quality assessment variables (Status_QA) and sun-sensor geometry. Description of the dataset attributes was given in Table 4.

Table 5: EPIC MAIAC Product Suite

Dataset ID	Data type	Scaling factor	Description
Sur_refl_Lamb_xxx,	16-bit integer	0.0001	Atmospherically corrected surface reflectance. xxx stands for the wavelength (340, 388,443, 551, 680, 780 nm)
BRF_xxx	16-bit integer	0.0001	Atmospherically corrected surface reflectance without Lambertian assumption. xxx stands for the wavelength (443, 551, 680, 780 nm)
Toa_refl_xxx	16-bit integer	0.0001	TOA reflectance. xxx stands for the wavelength (443, 551, 680, 780 nm)
Cloud_mask	8-bit integer	N/A	Cloud mask
Land_water_mask	8-bit integer	N/A	Land/water mask
AOD_443 AOD_551	16-bit integer	0.001	Aerosol optical depth (standard algorithm) at 443 nm and 551 nm
AOD_4D	16-bit integer	0.001	Aerosol optical depth at 443 nm generated by 4D retrieval
ALH	32-bit float	N/A	Aerosol layer height in km above ground level
AODSmkDust_xxx	16-bit integer	0.001	Aerosol optical depth (4D) for smoke and dust at 340, 388, 443, 551, 680, 780 nm
Fine_mode_frac551	16-bit integer	0.0001	Aerosol fine mode fraction (ocean only)
Angstrom_Exp_443-780	16-bit integer	0.0001	Angstrom exponent at 443-780 nm (ocean only)
Ref_Im_680	16-bit integer	0.0001	Imaginary refractive index for 680nm

SAE	16-bit integer	0.001	Spectral Absorption Exponent
SSA_xxx	16-bit integer	0.0001	Aerosol single scattering albedo at 340, 388, 443, 551, 680, 780 nm
NDVI_runAv	16-bit integer	0.0001	Running average of NDVI
NDVI_wRefl_update	16-bit integer	1	Update date for NDVI. Over water, it is the update date of water-leaving reflectance
Solar_zen_angle, Solar_az, View_zen_angle, View_az	32-bit float	1.0	Solar zenith, view zenith, solar azimuth, and view azimuth angles
Kiso_xxx, Kvol_xxx, Kgeo_xxx	16-bit integer	0.0001	The sRTLS BRDF model parameters for each spectral band (land only). xxx stands for the wavelength (443, 551, 680, 780 nm)
WaterL_Refl_388_runAv WaterL_Refl_340_runAv	16-bit integer	0.0001	Running average of water leaving reflectance at 388 and 340 nm
Status_QA	8-bit integer	N/A	Quality assessment
FminAbs	16-bit integer	0.0001	Fitting residual of 4D smoke/dust retrievals
Sigma381	16-bit integer	0.0001	Internal use
VF_Comp1	32-bit float	N/A	Black carbon (BC) volume fraction in smoke aerosols, or hematite volume fraction in dust aerosols
MC_Comp1	32-bit float	N/A	Column-integrated mass concentration (mg m^{-2}) of black carbon (BC) for smoke aerosols, or hematite for dust aerosols.
VF_Comp2	32-bit float	N/A	Brown carbon (BrC) volume fraction in smoke aerosols, or goethite volume fraction in dust aerosols
MC_Comp2	32-bit float	N/A	Column-integrated mass concentration (mg m^{-2}) of brown carbon (BrC) for smoke aerosols, or goethite for dust aerosols.
SRC	16-bit integer	0.001	Spectral Regression Coefficient for aerosol retrievals

5.5. Quality assessment dataset

Quality assessment variable, Status_QA, includes quality control information of the EPIC MAIAC algorithm performance. Detailed description of the QA definition is given in Table 5.

Table 6: Description of EPIC MAIAC QA

QA	Description
0	Best quality
1	Clear water, sediments detected
2	Clear, 1 neighbor cloud
3	Clear, more than 1 neighbor cloud
4	No retrieval
6	Height > 3.5 km, use climatology AOD=0.02
8	Sun glint
9	Land/water misclassification
10	No retrieval over water, CoxMunk glint reflectance too high
255	Fill value

Table 7: Cloud Mask definition

Cloud Mask value	Description
1	Clear
2	Possibly cloud
4	Cloud
6	Cloud shadow
7	Clear, smoke detected
8	Clear, dust detected
9	Clear, water sediments detected
10	Clear, water
13	Glint
15	Missclassified land/water
50	Undefined
255	Fill Value

Table 8: Land/Water Mask

LWS Mask value	Description
1-3	Land
4	Snow
5	Ice on water
6	Water
7	Deep Water
8	Shallow Sea
9	Static Sea
10	Static Lake
255	Fill value

6. ANALYSIS AND VALIDATION OF MAIAC PRODUCTS

6.1 Data Availability

The retrieval availability is defined as ratio of the number of valid retrievals to the total number of pixels. Both the temporal and spatial variation of the global aerosol retrieval availability is analyzed.

Figure 4 (left) shows the global aerosol retrieval availability for one year (2016) as a function of time. For most days in 2016, the data availability ranges from 15% to 27%, reaching the maximum during the northern hemisphere summer. This is consistent with the fact that 1) EPIC provides about two times more observations per day during the northern hemisphere summer than during the winter; 2) land coverage over snow-free area, where aerosol retrievals can be performed, increases at northern latitudes during the summer season.

Figure 4 (right) shows spatial variation of AOD retrieval availability for 2016. Clearly, there are (1) more retrievals over the land than over the ocean; and (2) AOD retrieval availability negatively correlates with cloudiness and snow cover.

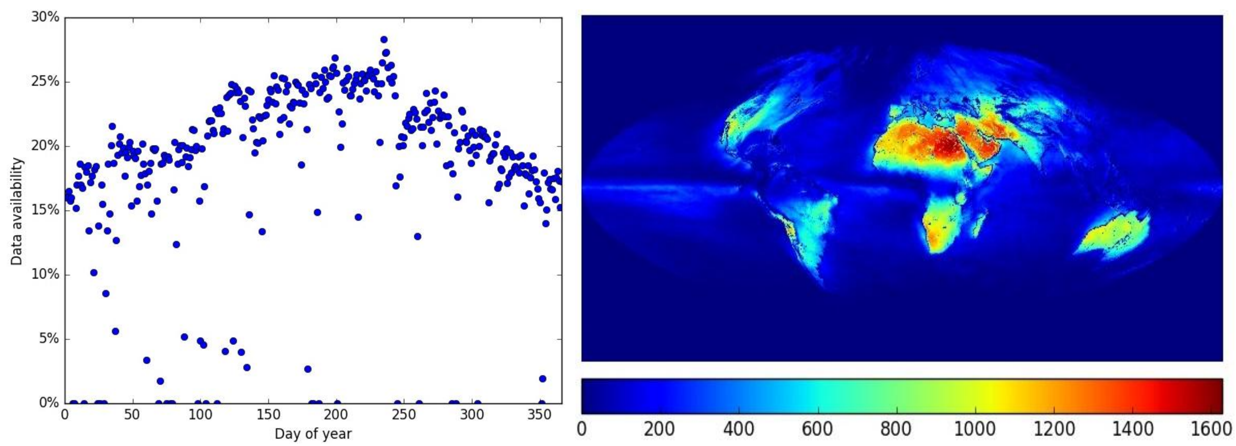

Figure 4. The annual variation of EPIC MAIAC aerosol optical depth retrieval availability (left) and spatial distribution of total number of valid EPIC MAIAC AOD retrievals during 2016.

6.2 Validation

6.2.1. Standard Algorithm

EPIC MAIAC AOD *from standard retrievals* was validated globally using AERONET data for all available sites (Lyapustin et al., 2021). EPIC AOD is calculated as a mean value in the 5x5 window (50km) centered on each site and within ±30 minutes of AERONET observations.

The results of AERONET $AOD_{0.44}$ validation are shown in Figure 5. The EPIC data were filtered according to the Sun and view zenith angles less than ~63° and at least 50% coverage in the spatial window. The site-level global statistics shows the correlation coefficient (R), root mean square error (RMSE) and the mean bias error (MBE, MAIAC–AERONET). MAIAC shows a good retrieval accuracy, with R ≥ 0.7–0.8 and low RMSE and MBE, over vegetated parts of the world including North and South America, north-central Eurasia and Oceania. AOD is generally overestimated over bright surfaces such as western United States and Australia. Such bias is typical for aerosol products based on a single-view satellite measurement, and it is exacerbated for EPIC due to unfavorable view geometry near the backscattering direction. The underestimation of AOD is obvious in regions of strong biomass burning, including central Africa, Indo-Gangetic plain and south Asia. Similar to the bias, the RMSE is generally low globally with the exception of the major dust and biomass burning aerosol source regions which also have a much higher annual average AOD. The correlation is generally high in regions with higher magnitude and variability of AOD. On the contrary, the low correlation is observed over regions with low aerosol loading and low natural variability, such as Australia or south of the South American continent. The two scatterplots on the right summarize the global validation analysis. The left one 1) shows all AERONET sites. On the right scatterplot (b), we excluded 11 bright surface sites over the Western United States (Bakersfield; Goldstone; KeyBiscayne; Neon_ONAQ; Railroad Valley; Sandila_NM_PSEL; TableMountain_CA; Tucson; UACJ_UNAM_ORS; White_Sands_HELSTF; Yuma) and one site over Australia (Birdsville). These sites are located in arid regions with low AOD and low AOD variability where MAIAC EPIC overestimates AOD and shows low R-values. Due to low cloudiness, these sites also contribute a disproportionate ~9% of the total matching points. Considering the right scatterplot as a baseline, MAIAC shows an overall correlation of 0.77 with RMSE ~0.159 and a mean bias of 0.046. Over 66.72% of MAIAC EPIC AOD agree with AERONET within the expected error (EE) of ±(0.1 + 0.1AOD).

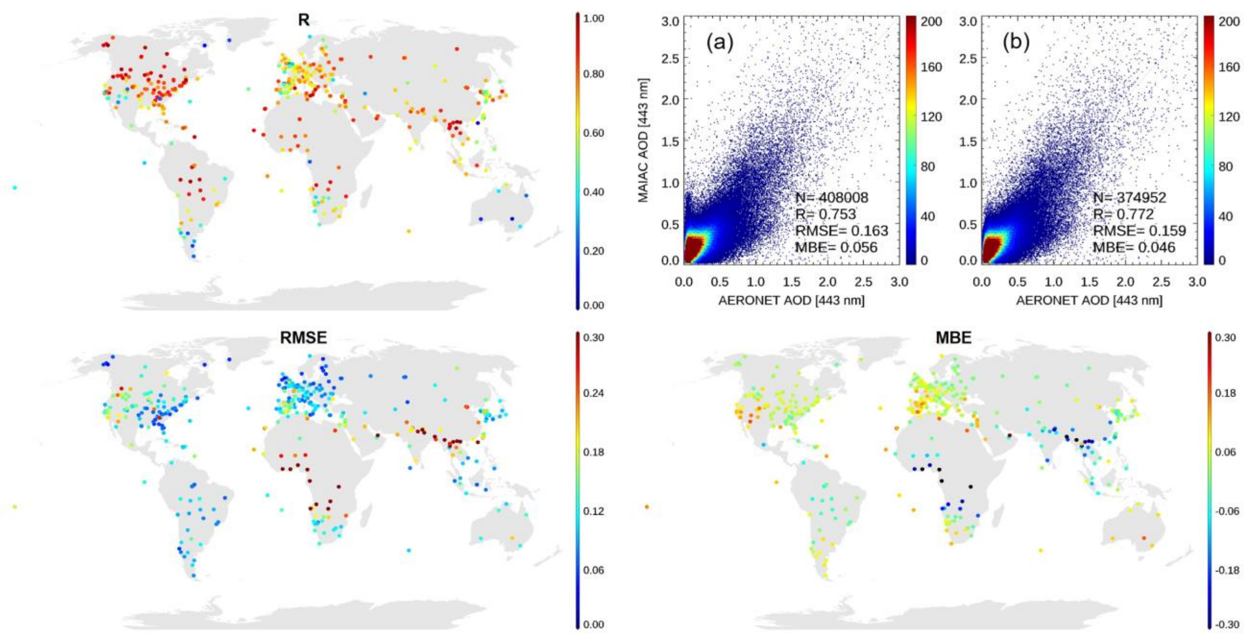

Figure 5. Global AERONET validation of MAIAC EPIC AOD at 443 nm (adapted from Fig. 2 of Lyapustin et al., 2021a). The geographic distribution of the site-level results is displayed for the regression coefficient (R), root mean square error (RMSE) and the mean bias error (MBE). The two scatterplots show the summary validation using (A) all AERONET sites and (B) all sites without 12 bright sites with low AOD and low variability.

6.2.2. Advanced (4D) Aerosol Retrievals

To yield a globally representative accuracy assessment, we used a 2015-2024 EPIC data record re-processed with v3 MAIAC algorithm and performed validation of derived aerosol optical properties and layer height using AERONET and CALIOP (up to August 2023) data, respectively (Lyapustin et al., 2025). The MAIAC expected error for AOD is defined as $EE = \pm(0.05 + 0.2 \times$ AERONET AOD) for AOD_{443} and as ±0.03 for the single scattering albedo, which is the stated uncertainty of AERONET inversion-based SSA (Sinyuk et al., 2020).

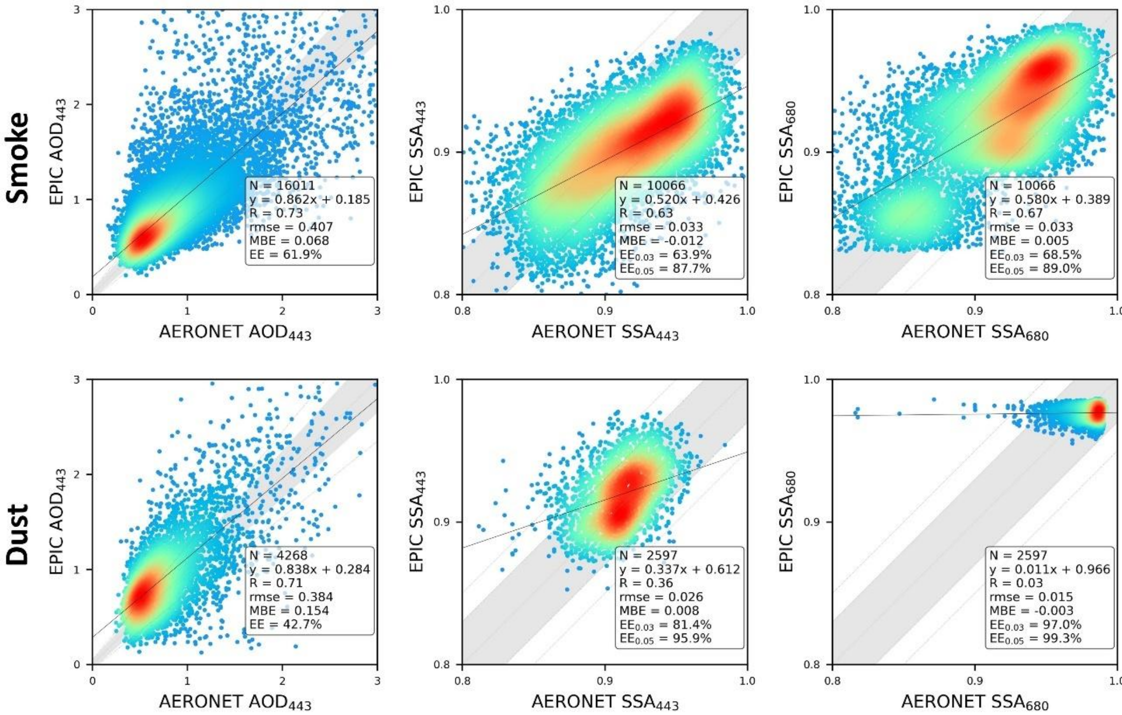

Figure 6. Global AERONET validation of aerosol optical depth (AOD_{443}) and spectral single scattering albedo at 443 and 680 nm for smoke (top) and mineral dust (bottom) (adapted from Fig. 3 of Lyapustin et al., 2025).

Figure 6 shows that the v3 algorithm retrieves aerosol optical properties with good accuracy. The AOD has a correlation coefficient *R*~0.71-0.73 and *RMSE*~0.4. The mean AOD *bias* is positive for both smoke (0.07) and dust (0.15). Partly responsible for this bias is the EPIC view geometry near the exact backscattering, where the surface brightness increases often significantly due to the lack of shadows (called 'hot spot', e.g. Ross and Marshak, 1989). While the AOD retrieval accuracy is average, the achieved global accuracy of spectral absorption is very good. The SSA correlates well with AERONET values, in particular for smoke (R~0.63-0.67), and shows low *RMSE*~0.02-0.03 and constrained mean *bias* within approximately ±0.01. Importantly, about 64-69%/81-97% of SSA values for smoke/dust aerosols match AERONET SSA within uncertainty of ±0.03.

A global CALIOP-based validation of MAIAC EPIC ALH, based on the entire EPIC-CALIPSO overlap period of July 2015 – August 2023, is shown in Figure 7. The results, displayed separately for smoke and dust aerosols over the land and over the ocean show good accuracy. ALH has a low global *RMSE*~1.1 km, no *bias* over the ocean, and relatively low *bias* of -0.45 km for smoke and -0.75 km for dust over land. The bias may reflect the difference between EPIC ALH representing optical centroid, and backscatter-weighted mean height from CALIOP.

Between 77% over land and 63% over ocean of smoke ALH values are within *EE*=±1 km from CALIOP ALH_C. The numbers are similar for dust, from 60% over land to 75.5% over ocean are within *EE*=±1 km.

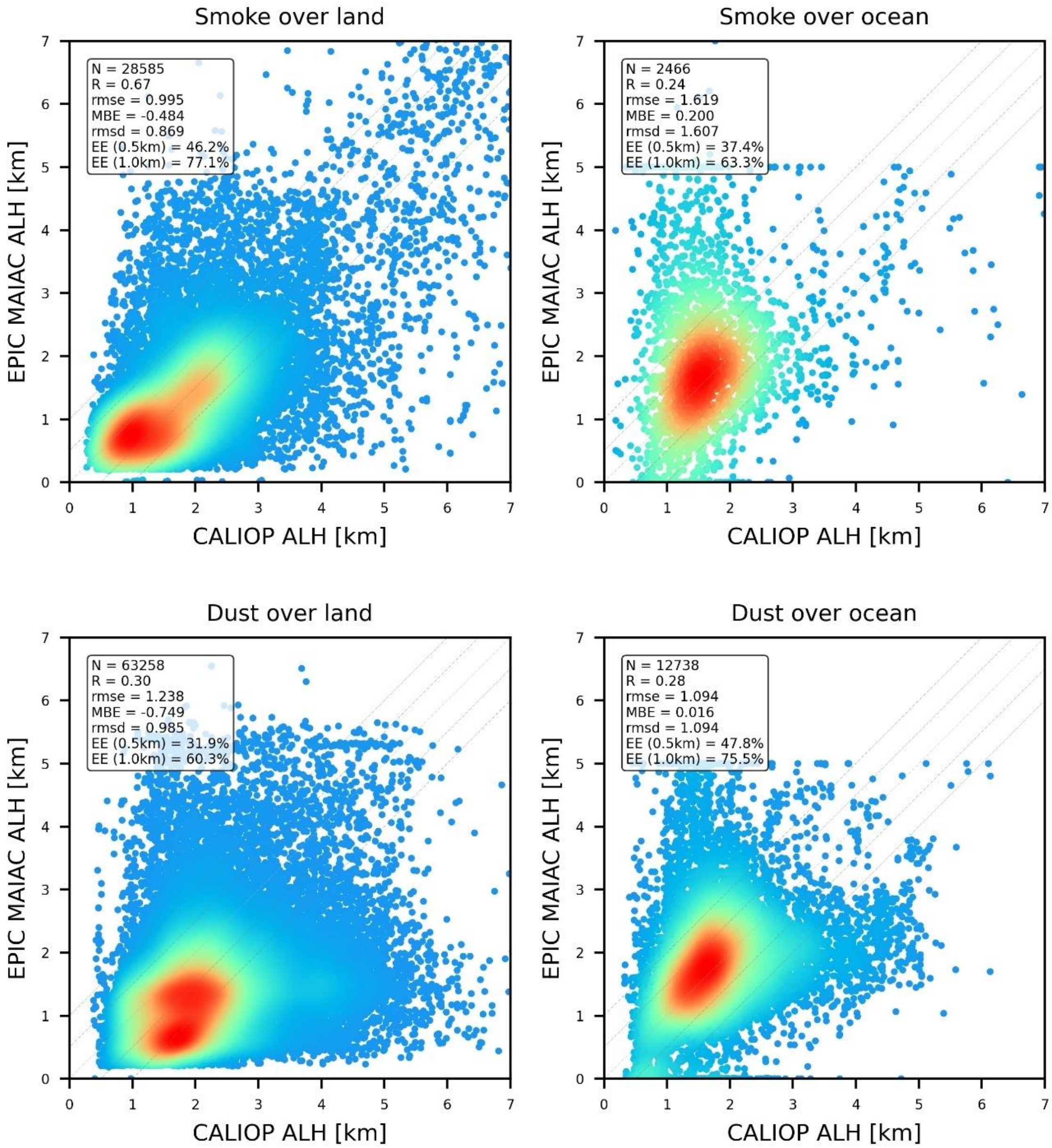

Figure 7. Global CALIOP CALIPSO validation of v3 MAIAC EPIC aerosol layer height over the land and the ocean for smoke (top) and mineral dust (bottom) (adapted from Fig. 4 of Lyapustin et al., 2025).

DATA AVAILABILITY STATEMENT

The v3 MAIAC EPIC products are available for downloading from the Atmospheric Science Data Center (ASDC) at NASA Langley Research Center (Available at: https://doi.org/10.5067/EPIC/DSCOVR/L2_MAIAC.002).

ACKNOWLEDGEMENTS

This work was funded by the NASA DSCOVR program (managers R. Eckman and E. Knowland). We are grateful to NASA DSCOVR Project providing high quality calibrated and geolocated (L1B) EPIC data and to the NASA Center for Climate Simulations used for EPIC data processing.